BRINKMAN-EXTENDED DARCY FLOW IN METAL FOAM: ANALYSIS AND EXPERIMENT

Dukhan, N.*
*Author for correspondence
Department of Mechanical Engineering,
University of Detroit Mercy,
Detroit, MI 48221
USA
E-mail: nihad.dukhan@udmercy.edu

ABSTRACT

Fluid flow in porous media is found in numerous processes and applications of vital engineering interest, e.g., storage of nuclear waste, heat exchangers, ground water pollution and chemical reactors. Often, the porous medium is confined by solid boundaries for containment. These impermeable boundaries give rise to shear stress and boundary layers. The Brinkman-extended Darcy equation governs the momentum transport due to Newtonian fluid flow in such porous-media flow situations. Metal foam, especially aluminum-based, has gained a lot of academic and industrial interest over the past few years. The significance of metal foam is due to its low density (or, high porosity: 75 % to 95 %.), high thermal conductivity, interconnectivity of its solid ligaments and large surface area density. Metal foam applications include heat exchange system and chemical reactors. In these systems, the foam is usually cylindrical in shape and is contained in a cylindrical tube. The fluid flow in such systems is needed for further engineering and performance analysis of such systems. The flow field may be described by the Brinkman-extended Darcy equation. This equation is solved analytically in a cylindrical system, employing an existing fully-developed boundary-layer concept particular to porous media flows. As expected, the volume-averaged velocity is found to increase as the distance from the boundary increases reaching a maximum at the center. The friction factor is defined based on the mean velocity and is found to be inversely proportional to the Reynolds number, the Darcy number and the mean velocity. In order to check the validity of the Brinkman-extended Darcy flow model for the high-porosity metal foam, experiments were conducted on commercially-produced 20-ppi (pores per inch), i.e., 8 pores per centimeter using an-open loop wind tunnel. In the Darcy flow regime, reasonably good agreement is found between the analytical and the experimental friction factors. The implication of the results of this paper is that they can be applied in further engineering analysis that require knowledge of the velocity field and pressure drop, i.e., convection heat transfer and chemical reactors.

INTRODUCTION

Open-cell metal foam is a class of modern porous media that possesses large accessible surface area per unit volume and high porosities (often greater than 90%). These properties make the foam attractive for certain devices such as catalytic systems, heat exchanges and chemical reactors. The internal structure of the foam is web-like formed by connected ligaments. Flow fields in such structure are rather complex and include flow reversal and vigorous mixing. The penalty is an increase in pressure drop. However, this increase can be mild and the foam can compete with the most existing cores.

NOMENCLATURE

Da	[-]	Darcy number
f	[-]	Friction factor
I	[-]	Modified Bessel function
K	[m^3]	Permeability
r	[m]	Radial coordinate
r_o	[m]	Radius of cylindrical porous medium
R	[m]	Non-dimensional radial coordinate
Re	[-]	Reynolds number
p	[Pa]	Static pressure
w	[m/s]	Volume-averaged velocity
W	[-]	Non-dimensional velocity
z	[m]	Axial coordinate along the flow direction
Z	[-]	Non-dimensional axial coordinate

Special characters

β	[-]	Ratio of dynamic viscosity to effective viscosity
δ	[-]	Uncertainty
Δ	[-]	Change
ε	[-]	Porosity
μ	[N.s/m^2]	Fluid dynamic viscosity and the heat-generating medium
ρ	[kg/m^3]	Density of fluid
ω	[-]	Non-dimensional parameter

Among the important characteristics of porous media flows are the velocity profile and pressure drop. For example, the velocity profile directly influences convection heat transfer in heat exchangers, the reaction rate in chemical reactors and the rate of deposit materials in filters. The pressure drop dictates the required pumping power needed for these operations.

Because of the internal geometry and the complex flow filed, exact solutions of the complete transport equations inside porous media including the foam are scarce. Researchers have relied heavily on numerical solutions and to some extend on analytical solutions of simplified forms of the governing equations, e.g., Poulikakos and Renken [1], Amiri and Vafai [2], Calmidi and Mahajan [3] and Angirasa [4].

When the porous medium is bounded by a solid surface, the wall shear stress is included in the well-known Darcy equation. The inclusion of the wall shear stress in the momentum equation is attributed to Brinkman, and the name of the momentum equation changes to Darcy-Brinkman [5, 6].

Vafai and Tien [7] analyzed the flow and heat transfer in a porous medium next to a solid boundary; they showed that neglecting the boundary effects could lead to significant errors in heat transfer calculations. Poulikakos and Kazmierczak [8] analytically studied forced convection and fluid flow in a duct partially filled with a porous medium. Two geometries were investigated parallel plates and a circular pipe. In both cases, the porous medium was attached to the solid wall. The Darcy-Brinkman model was used inside the porous medium.

Haji-Sheikh and Vafai [9] provided analysis of heat transfer in porous media imbedded inside ducts formed by circular tube or parallel plates. As part of the heat transfer analysis, they briefly presented the solution to the Darcy-Brinkman equation. The same hydrodynamic analysis was used by Minkowycz and Haji-Sheikh [10].

The present paper presents analysis for Newtonian fluid flow in confined cylindrical porous media. The cylindrical geometry is widely used in some actual porous media designs, e.g., heat exchange systems and chemical reactors. The solution was verified by experiments on a sample of metal foam.

ANALYSIS

A porous-media-filled circular tube of radius r_o is shown schematically in Fig. 1. There is fully-developed one-dimensional flow of a Newtonian fluid in the z-direction with a volume-averaged velocity component w. A boundary layer employed in the current analysis is a special kind of boundary layers unique to porous media flows, and was conceived first by Vafai and Tien [7]. Unlike the traditional boundary layers for open pipe flow, this boundary layer is fully-developed and does not grow in the flow direction due to the internal structure of porous media. The Brinkman-extended Darcy momentum equation inside the boundary layer is

$$\frac{dp}{dz} = -\frac{\mu}{K}w + \frac{\mu_e}{r}\frac{d}{dr}\left(r\frac{dw}{dr}\right) \tag{1}$$

where μ is the fluid viscosity and K is the permeability of the porous medium. The effective viscosity μ_e is a function of the dynamic viscosity of the fluid and the geometry of the porous medium. The ratio μ/μ_e has been set equal to 1 [5, 6]. Nield and Bejan [5] pointed out that this was not true in general, and they stated that μ/μ_e has been set μ/μ_e equal to 0.13 for high-porosity rigid foam. Kaviany [6] gave a range for from 0.28 to 1 according to $\beta = 1/[1 + 2.5(1 - \varepsilon)]$, where ε is the porosity.
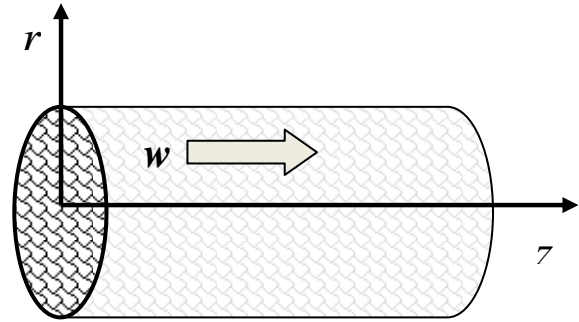
Figure 1 Schematic of the confined cylindrical porous-media system

Outside the boundary layer, the momentum equation simplifies to

$$\frac{dp}{dz} = -\frac{\mu}{K}w_\infty \tag{2}$$

where w_∞ is the volume-averaged free-stream velocity outside the boundary layer. The boundary conditions are

$$at \ r = 0 \quad \frac{dw}{dr} = 0 \tag{3}$$

$$at \ r = r_o \quad u = 0 \tag{4}$$

Combining the two momentum equations in a non-dimensional form, and rearranging

$$R^2\frac{d^2W}{\partial R^2} + R\frac{dW}{dR} - \frac{\beta}{Da}R^2(W - 1) \ = \ 0 \tag{5}$$

with the boundary conditions

$$at \ R = 0 \quad \frac{dW}{dR} = 0 \tag{6}$$

$$at \ R = 1 \quad W = 0 \tag{7}$$

where $R = r/r_o$, $Da = K/r_o^2$ (the Darcy number), $\beta = \mu/\mu_e$ and $W = w/w_\infty$. The permeability, and hence the Darcy number, can be determined from reliable models or experimental data provided in the literature. Models for metal foam's permeability include those of Du Plassis et al. [11], Fourie and Du Plassis [12], Bhattacharya et al. [13]. Experimental values of the permeability of metal foam can be found in studies such as those of Calmidi and Mahajan [3], Antohe et al. [14] and Lage, et al. [15].

The solution to Eqs. (5) through (7) is obtained by comparing the differential equation to the general form of Bessel equation [16], and applying the two boundary conditions:

$$W = 1 - \frac{I_o(\omega R)}{I_o(\omega)} \qquad (8)$$

where $\omega = \sqrt{\beta/Da}$ and I_o is the modified Bessel function of order zero.

The non-dimensional mean velocity is obtained by integrating the velocity over the cross-sectional area according to:

$$W_m = \frac{1}{\pi}\int_0^1 \left[1 - \frac{I_o(\omega R)}{I_o(\omega)}\right]2\pi R dR = 1 - \frac{2I_1(\omega)}{\omega I_o(\omega)} \qquad (9)$$

where $W_m = w_m/w_\infty$ and the integral $\int x I_o(x)dx = x I_1(x)$ was employed. As ω increases the mean velocity approaches unity, meaning the physical mean velocity is approximately equal to the free stream velocity. This is expected, since the boundary layer is rather thin for large ω and the free stream velocity prevails over most of the cross section. As an engineering approximation, one may set the free-stream velocity equal to the mean velocity for large values of omega. This has a practical advantage since the mean velocity through confined porous media can be measured.

The friction factor can be defined and obtained as

$$f \equiv \frac{-(\partial p/\partial z)D}{\rho w_m^2/2} = \frac{8}{W_m Da Re} \qquad (10)$$

where $Re \equiv \rho w_m D/\mu$. The pressure drop of Eq. (2) was employed. The expression of the non-dimensional mean velocity of Eq. (9) can be substituted into Eq. (10), which gives a relationship between the friction factor, ω, Da and Re.

EXPERIMENT

A sample of open-cell aluminium foam commercially available (ERG Materials and Aerospace) was used to verify the analytical results. The sample was made from aluminium alloy 6101-T6, and had 10 pores per linear inch (ppi). Properties of the samples used in this experiment are given in Table 1. A photograph of the sample in the test sections is shown as Fig. 2 The sample was cylindrical in shape and had a diameter of 8.89 cm and a length of 15.24 cm (6.0 in) in the flow direction. For this length the entrance/exit effects are negligible [17].

Table 1 Foam parameters

Porosity $\varepsilon\%$	Permeability, K X 10^7, m^2	Parameter ω	Darcy Number, Da X 10^4
89.5	3.65	65.45	1.84

Figure 2 Photograph of the foam sample in its test section

Experiments were performed in an open-loop wind tunnel shown schematically in Fig. 3. A suction unit which could produce air flow rates up to 17 m^3/min (600 ft^3/min) was used to induct room air into the tunnel and through the foam sample. A variable flow controller provided adjustment of the airflow through the tunnel.
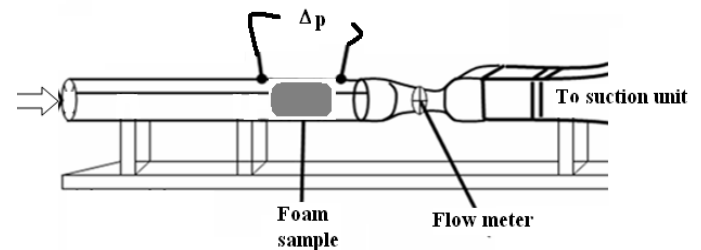
Figure 3 Schematic of the experimental set-up

The test section of the tunnel was fabricated from thin Plexiglas tubes with internal diameter that matched the sample's diameter with a tight tolerance, Fig. 2. The test section was placed securely and sealed between two circular ducts having the same inner diameter. The upstream duct had a length greater than ten times the diameter of the test section to reduce the duct's entrance effect at the test section. The tunnel entrance had a plastic screen having a fine mesh (with a screen open-area ratio = 0.53) to minimize any large structures in the room air.

Two holes were drilled at the top of the test section, one before and one after the test section at a distance of 2.54 cm (1 inch). The holes hosted pressure measurement tubing. The pressure drop was measured using an Omega differential pressure transmitter with a range 0 to 746 Pa (0 to 3 in H$_2$O).

For velocity measurement, an Extech gas flow meter that could measure speeds up to 35 m/s (29 ft/min) was used. The pressure transducer and the flow meter were connected to a data acquisition system (DAQ by Omega Engineering) which delivered the readings to a computer.

The flow rate was varied to realize different velocities in the test section. For each velocity, the steady-state static pressure drop was measured using the pressure taps and the differential pressure transducer.

For gas flow in porous media, the pressure drop is usually significant such that compressibility effects may become important. Thus in order to account for variations in gas density, the pressure drop was computed using the following

$$\Delta p = \frac{p_i^2 - p_o^2}{2 p_i} \qquad (11)$$

where p_i and p_o are the inlet and exit pressures, see for example Bonnet et al. [18].

Uncertainty Analysis

The uncertainty in the velocity measurement had a contribution from a fixed error, $e_f = 2\%$ (provided by the manufacturer) and a random estimated error, $e_r = 10\%$ in each reading. For the pressure transducer e_f was 5% and e_r was 7% (these were provided in a calibration certificate). The total uncertainties in the pressure and velocity were calculated by the root-sum-squares method according to Figliola and Beasley [19], which resulted in a total uncertainty in the pressure drop $\delta_{\Delta p}$ of $\pm 8.6\%$, and in the air velocity δ_{u_m} of $\pm 10.2\%$. The length and diameter of each sample were measured using a calibre. The uncertainties in these readings were $\delta_L = \delta_D = 0.5$ mm.

Further uncertainty analysis was performed in order to assess how the uncertainties in the measured variables propagate into the uncertainty in each computed variable, i.e., the uncertainties in the calculated values of friction factor, f, and the Reynolds number, Re. The following uncertainties in f and Re are obtained $\left(\delta_f / f\right) = \pm 14.7\%$ and $\delta_{Re}/Re = \pm 10.4\%$.

COMPARISON TO EXPERIMENTAL RESULTS

The experimental results are compared to the prediction of the analytical solution given by Eq. (10) in the form of friction factors. For each sample, the experimentally obtained friction factor was calculated form experimental values according to its definition $f \equiv -\left(\partial p / \partial z\right) D / \rho u_m^2 / 2$. The Reynolds number for each sample was calculated using the measured mean velocity and the sample's diameter.

The parameter ω was then calculated according to its definition $\omega = \sqrt{\beta / Da}$, which allowed the non-dimensional velocity to be computed according to Eq. (9). The ration β was obtained from [6]. Using ω, the Darcy number and the experimental values of Reynolds number, the analytical value of the friction factor was obtained according to Eq. (10).

Figure 4 shows a comparison of the analytical and experimental friction factors at the same Reynolds number. The experimental friction factor seems to divert from the analytical prediction for values of Reynolds number greater than about 2800. It is very likely that this value of Reynolds number marks the end of the Darcy flow regime, and the beginning of a transition towards the Forchheimer regime.
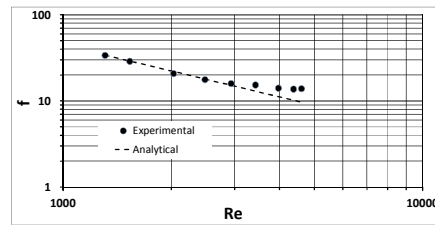
Figure 4 Analytical and experimental friction factor versus Reynolds number

CONCLUSION

The Brinkman-Darcy equation was solved for the velocity as a function of the radial distance from the centre of a cylindrical porous tube. For low Darcy number (small diameter and/or high permeability), the velocity was constant over most of the cross section. Hence, the average velocity can be taken to be approximately equal to the free-stream velocity. These trends are the result of the fact that the thickness of the boundary layer is rather small when the Darcy number is small. The friction factor depended on the Reynolds number to the power -1. According to the analytical results, at a given Reynolds number, the friction factor increased with the ratio of actual to effective viscosity and decreases with Darcy number. These two parameters are governed by the porosity and diameter of a cylindrical porous medium. The analytical results were verified by experiments utilizing aluminium foam. Reasonably good agreement between the analytical and experimental friction factor, strictly in the Darcy regime, was obtained. The current solution can be useful in further flow, heat transfer and reactor analyses that deal with Darcy flow in porous media.

REFERENCES

[1] Poulikakos, D. and Renken, K., 1987, "Forced Convection in a Channel Filled with Porous Medium, Including the Effect of Flow Inertia, Variable Porosity, and Brinkman Friction," ASME J. Heat Transfer, 109, pp. 880-888.

[2] Amiri, A. and Vafai, K., 1994, "Analysis of Dispersion Effects and Non-Thermal Equilibrium, Non-Darcian, Variable Porosity Incompressible Flow through Porous Media," Int. J. of Heat and Mass Transfer, 37(6), pp. 939-954.

[3] Calmidi, V. V. and Mahajan, R. L., 2000, "Forced Convection in High Porosity Metal Foams," ASME J. Heat of Transfer, 122, pp. 557-565.

[4] Angirasa, D., 2002, "Forced Convective Heat Transfer in Metallic Fibrous Materials," ASME J. of Heat Transfer, 124, pp. 739-745.

[5] Nield, D.A. and Bejan, A., 1992, Convection in Porous Media, 2nd Ed., Springer, New York, NY, pp. 12.

[6] Kaviany, M., 1991, Principal of Heat Transfer in Porous Media, Springer, New York, NY, pp.52,70,94.

[7] Vafai, K. and Tien, C. L., 1981, "Boundary and Inertia Effects on Flow and Heat Transfer in Porous Media," Int. J. of Heat and Mass Transfer, 24(8), pp. 195-203.

[8] Poulikakos, D. and Kazmierczak, M., 1987, "Forced Convection in a Duct Partially Filled with a Porous Medium," ASME J. of Heat Transfer, 109, pp. 653-662.

[9] Haji-Sheikh, A. and Vafai, K., 2004, "Analysis of Flow and Heat Transfer in Porous Media Imbedded Inside Various-Shaped Ducts," Int. J. of Heat and Mass Transfer, 47, pp. 1889-1905.

[10] Minkowycz, W. J. and Haji-Sheikh, A., 2006, "Heat Transfer in Parallel Plates and Circular Porous Passages with Axial Conduction," Int. J. of Heat and Mass Transfer, 49(13-14), pp. 2381-2390.

[11] Du Plassis, P., Montillet, A., Comiti, J. and Legrand, J., 1994, "Pressure Drop Prediction for Flow through High Porosity Metallic Foam," Chemical Engineering Science, 49(21), pp. 3545-3553.

[12] Fourie, J. G. and Du Plassis, J. P., 2002, "Pressure Drop Modeling in Cellular Metallic Foams," Chemical Engineering Science, 57, pp. 2781-2789.

[13] Bhattacharya, A., Calmidi, V. V. and Mahajan, R. L., 2002, "Thermophysical Properties of High Porosity Metal Foams," Int. J. of Heat and Mass Transfer, 45, pp. 1017-1031.

[14] Antohe, B. V, Lage, J. L., Price, D. C. and Weber, R. M., 1997, "Experimental Determination of Permeability and Inertia Coefficients of Mechanically Compressed Aluminum Porous Matrices," ASME J. of Fluids Engineering, 119, pp. 404-411.

[15] Lage, J. L., Antohe, B. V. and Nield, D. A., 1997, "Two Types of Nonlinear Pressure-Drop versus Flow-Rate Relation Observed for Saturated Porous Media," ASME J. of Fluids Engineering, 119, pp. 700-706.

[16] Myers, G.E., 1998, Analytical Methods in Conduction Heat Transfer, 2nd Ed., AMCHT Publications, Madison, WI, pp. 46.

[17] Dukhan, N. and Patel, K., 2011, "Effect of Sample's Length on Flow Properties of Open-Cell Metal Foam and Pressure-Drop Correlations," J. of Porous Materials, 18(6), pp. 655-665.

[18] Bonnet, J.-P., Topin, F. and Tadrist, L., 2008, "Flow Laws in Metal Foams: Compressibility and Pore Size Effects," Transport in Porous Media, 73, pp. 233-254.

[19] Figliola, R. and Beasley, D., 2000, Theory and Design for Mechanical Measurements, John Wiley and Sons, New York, NY, pp. 149-163.